Chapter 3

Large Power factor and Anomalous Hall effect and their correlation with observed linear magneto resistance in Co-doped Bi_2Se_3 3D Topological Insulator

3.1: INTRODUCTION

In recent years Topological Insulators (TI) have attracted much attention because of their novel properties arise from strong spin-orbit coupling and massless Dirac-cone like surface states protected by time reversal symmetry [17], [40]–[42].This confers on the surface state for its topological protection, i.e. the surface state remains gapless even in the presence of moderate disorder. The effort to break the topologically protected surface state by introducing magnetic ordering would enable to observe the quantized anomalous Hall Effect [43]–[45]. Among the various discovered TI materials Bi_2Se_3 is one of the most promising candidates as it has a single Dirac cone in the Brillouin zone and relatively large bulk energy gap of 0.3eV, sufficient for room temperature applications [18], [46]. Topological insulators will also be of interest for spintronic materials as the Dirac states can be used to carry the spin current with small heat dispersion [47], [48]. Furthermore, the development of ferromagnetism (FM) in Bi_2Se_3 will be more interesting in many ways: point charge induced magnetic monopole and topological contributions to the Faraday and Kerr magneto-optical effects. Ferromagnetism has been reported in several transition metal ion doped topological insulators, viz. in Cr, Fe, Cu doped Bi_2Se_3 [49], [50] V, Cr, Mn doped Sb_2Te_3 [51], [52]Fe and Mn doped Bi_2Te_3 [53], [54] Moreover, recently FM has been reported in Cr doped Bi_2Se_3 thin film . A hallmark of the presence of such FM is anomalous Hall effect [11], where Hall resistance shows a hysteresis loop behavior under magnetic field [55], [56]Furthermore, Bi_2Se_3 material is the potential candidate for Thermoelectric (TE) devices which are used for solid state cooling and power generation from waste heat. These devices use two types of semiconductor “legs”, n type and p type, connected in series. The performance of a TE material is evaluated by the Figure of merit $ZT=S^2/\rho k$, where S, ρ, and k are the Seebeck coefficient, electrical resistivity, and thermal

conductivity of the material respectively. An efficient TE material should posses high ZT. Worldwide there is resurgence in activity for revealing the underlying physics towards obtaining higher ZT. By maximizing the power-factor PF=S^2/ρ and/or lowering the thermal conductivity, efficiency of a TE device can be improved. On the other hand, recent studies [57]–[59]on magneto transport in two dimensional Bi_2Se_3 reveal a non-saturated, linear MR under strong field, which promises its potential applications in magnetic sensing. Tang et al [60]. Remarkably reveal that the linear MR is induced by a two-dimensional transport. Although the carrier concentration and mobility can be obtained from Shubnikov-de Haas oscillations at low temperatures, the Hall measurement cannot be carried out in their quasi-one dimensional device and the carrier mobility at high temperature is unknown. He et al [61] conduct a magnetotransport study on ultrathin film of Bi_2Se_3 with variable thickness grown by molecular beam epitaxy, which shows much smaller magnetoresistance (less than 10%) at 14 T. More recently, a linear magnetoresistance up to 80% is observed at 12 T [62]. Yan et al [63] have reported a large linear MR nearly 400% at low temperature and a corresponding high mobility of 10,000 cm^2V^{-1} s^{-1} in Bi_2Se_3nanoplate. The linear MR persists even at room temperature with the value of 75%.However, the MR in bulk Bi_2Se_3 and the relationship between the MR of Bi_2Se_3 and carrier mobility has still not been revealed. In fact, magnetoresistance (MR) of these materials gives valuable insight into the mechanism affecting conductivity, and hence is intimately related to the underlying physics towards obtaining materials with high TE values.

3.2: Synthesis of Materials

The single crystals of $(Bi_{1-x}Co_x)_2Se_3$ (with x=0, 0.04, 0.05, 0.06) were grown by modified Bridgeman method. We denoted the samples as 4%, 5% and 6% Co doped samples respectively for x=0.04, x=0.05 and x=0.06. The mixture of high purity (99.999%) Bi, Co and Se elements

were sealed in evacuated quartz ampoules. The ampoule was heated up to 920°C at 200°C per hour and was kept at that temperature for 12 hours and then it was slowly cooled to 550°C at the rate of 5°C per hour and hold there for 48 hours. Then it was cooled to room temperature at the rate of 10°C per hour. The crystals thus obtained were easily cleaved along the plane (00L) direction. X-Ray diffraction measurement was carried out using RigakuMiniFlex-II with Cu Kα radiation. The electrical transport properties were measured by using Quantum Design physical property measurement system (PPMS). The magnetic properties were measured using Quantum design magnetic property measurement system (MPMS).

3.3: RESULTS & DISCUSSIONS

3.3.1: X-Ray analysis

The X-ray diffraction pattern of all the samples is shown in Figure 3.1. According to this XRD study, all diffraction peaks correspond to the (00L) reflections of rhombohedral Bi_2Se_3, indicating that the cleaved surface is an *ab* plane with no secondary phases.

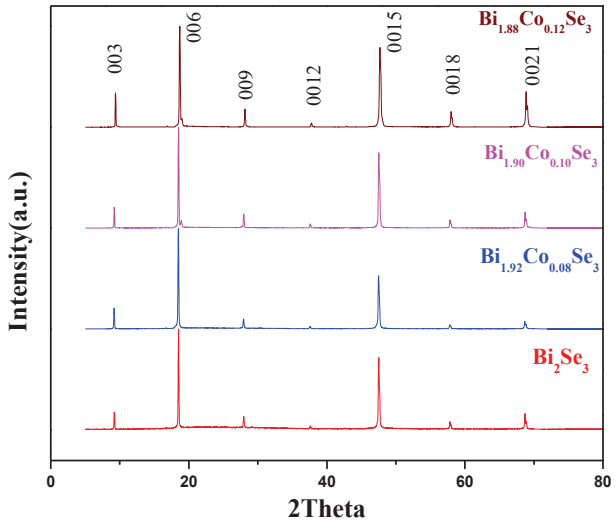

Figure 3.1: The X-ray diffraction patterns of $(Bi_{1-x}Co_x)_2Se_3$ (with x=0, 0.04, 0.05, 0.06).

3.3.2: Electrical Resistivity

The temperature dependence of resistivity of all the samples is shown in Figure 3.2a. Resistivity decreases monotonically indicating the metallic behavior. With Co doping the resistivity value increases. The impurity doping and application of large magnetic field may open a gap on the surface of the crystals. This is clearly evidenced at the low temperature resistivity data wherewith high doping concentration (6%) and with application of high magnetic field a clear upturn in the resistivity data is observed. Therefore, it can be pointed out that high doping and high magnetic field raise the Dirac cone above Fermi level and leaves a gap from the valence band. The magnetic field variation of band gap is shown in the inset of Figure 3.2a.

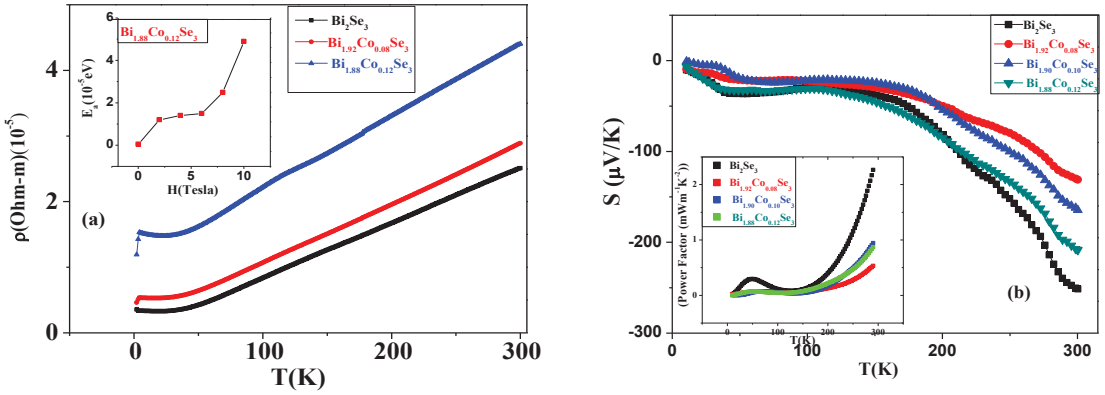

Figure 3.2: a) Temperature variation of resistivity of $(Bi_{1-x}Co_x)_2Se_3$ (with x=0, 0.04, 0.05, 0.06). Inset: The variation of band gap (which opens due to application of magnetic field) with external magnetic field of $(Bi_{0.94}Co_{0.06})_2Se_3$. (b) Temperature variation of Seebeck Coefficient of $(Bi_{1-x}Co_x)_2Se_3$ (with x=0, 0.04, 0.05, 0.06). Inset: The variation of power factor with temperature of $(Bi_{1-x}Co_x)_2Se_3$.

In this scenario, it is interesting to note the temperature variation of thermoelectric power, S(T) of the crystals (Figure 3.2b). Throughout the temperature region S value is negative, indicating that they are electron-doped. With increase of temperature, absolute value of S increases initially and above ~50K, it decreases marginally and then increases nearly monotonically, forming a broad hump-like feature. These S(T) features are consistent with earlier report [64].To determine the efficiency of thermoelectric power we have calculated the

power factor (shown in the inset of Figure 3.2b) of pure and undoped single crystal using the formula

$$\text{Power factor} = S^2/\rho \qquad (3.1)$$

Where, ρ is the electrical resistivity. In fact, the efficiency of any thermoelectric material can be evaluated by the term $ZT=S^2/\rho k$ [where, ZT represents the Figure of merit, k is the thermal conductivity]. To obtain the higher ZT, the S^2/ρ(power factor) should be maximized and k should be minimized. It has already been discussed that with increase of the temperature electrical resistivity is increasing in both pure and doped samples but the increase in Seebeck coefficient(S) is much larger than the increase of electrical resistivity which gives rise to the increase of power factor with increasing temperature. Since single crystal has been cleaved along basal plane, to find out a proper shape for the measurement of thermal conductivity was very difficult. Therefore, we could not perform thermal conductivity measurement for our samples. Hence we have estimated the PF and presented in the inset of Figure 3.2b as a function of temperature. It is observed that maximum PF is observed for undoped sample.

3.3.3: Magnetoresistance Analysis.

Figure 3.3 shows the magneto-resistance (MR) as a function of magnetic field at different temperatures of Co-doped Bi_2Se_3 samples. We have defined MR as $[\rho(H)-\rho(0)]/\rho(0)$. In fact, in pure Bi_2Se_3 at low magnetic field a curved behavior is observed which may indicate the weak antilocalization behavior (WAL) [65]–[67].This is the key feature of topological surface states, where Dirac Fermions travel around a self intersecting path or loop due to the spins rotating in opposite directions for the different paths forming an accumulated π-Berry phase. The destructive interference due to a π-Berry phase leads to a decrease of MR. An important aspect is

to observe the effect of incorporation of magnetic impurities in Topological Insulators. It is observed that the MR is exactly symmetric for all the samples (doped and undoped) with respect to the reversal of the field direction which rules out any possible contributions from the Hall voltage. Moreover, at low field MR shows a quadratic behavior and then transforms to linear variation with magnetic field without saturation. The linear and quadratic MR can be represented as:

$$MR=aH+bH^2 \qquad (3.2)$$

The variations of *a* and *b* with temperature are shown in Figure 3d. It is observed that with Co doping the quadratic term decreases appreciably at low temperature and for 6% Co doped sample the *b* value is negligible.

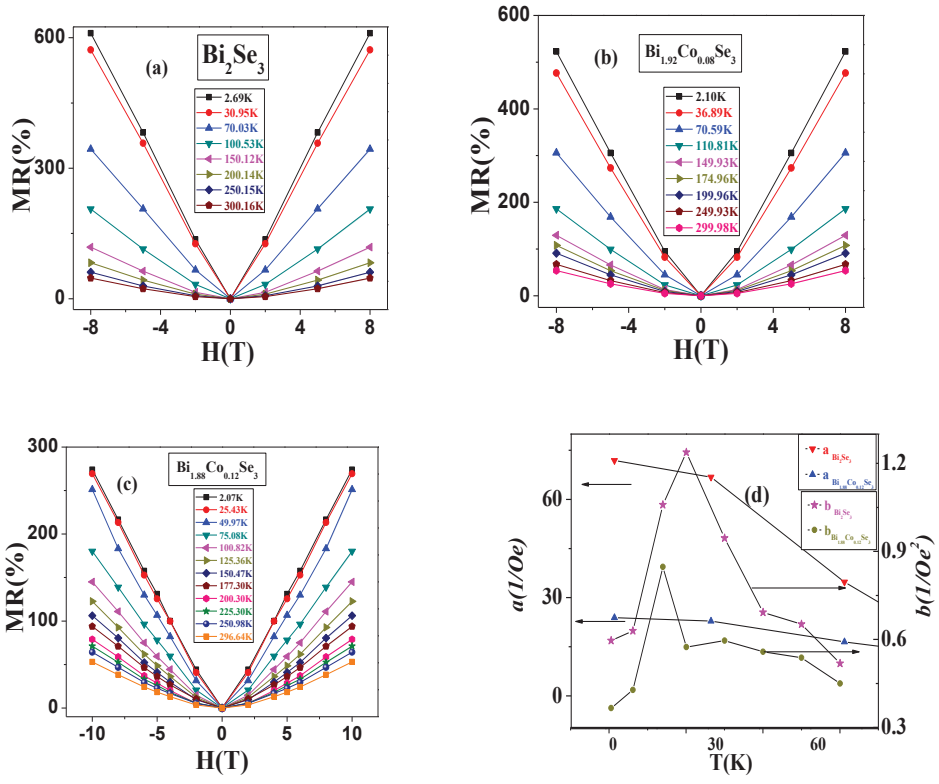

Figure 3.3: Magnetic field variation of magneto-resistance ratio of $(Bi_{1-x}Co_x)_2Se_3$ [with x=0 (a), 0.04 (b), 0.06 (c)] at different temperature. (d) Temperature variation of *a* and *b* parameters of $(Bi_{1-x}Co_x)_2Se_3$. We have shown the parameters for undoped and maximum doped samples.

Several mechanisms have been invoked to understand the linear MR part. Abrikosov et al. has proposed a quantum model for systems with a gapless linear dispersion spectrum [68] According to this model all the electrons are condensed into one Landau level when the "extreme quantum limit" $\hbar\omega_c > E_F$ ($\omega_c$is the cyclotron frequency) is satisfied. The maximum field can accurately be estimated using the inequality $n_0 < (eH/\hbar c)^{3/2}$. The carrier concentration obtained from the slope of hall resistivity is $\sim 10^{18}$, from where we estimated the magnetic field to be ~10T. But in the present case the value of the magnetic field (~2T) for Bi_2Se_3 is much lower than 10T. Moreover, in this model the MR is independent of temperature. Therefore, Abrikosov formula is not applicable throughout the measured temperature range for Bi_2Se_3.However, in a recent paper [69] Wang et al. have successfully explained the linear MR in Bi_2Te_3nano-sheet with Abrikosov model. Parish and Littlewood [70] proposed a model using the classical method which is applicable for the Bi_2Se_3 nanoplates [70]. According to this model the linear MR (LMR) arises because the local current density acquires spatial fluctuations in both magnitude and direction, as a result of heterogeneity or microstructure caused by non-homogeneous carrier and mobility distribution. Experimentally, in so many disordered systems [70], [71] the linear MR has been observed. Therefore, in the present investigation the LMR might be due to some disorderness. In Bi_2Se_3 sample the disorderness might be due to the *Se* vacancy. It is observed from the resistivity data that for doped samples a gap is opened at low temperature and also it is observed that at low temperature (below 25K) MR is independent of temperature. Therefore, at low temperature the LMR for the doped samples can be explained with the quantum model. As a matter of fact, there might be a transition from classical to quantum MR at low temperature with Co doping. It deserves further study. Moreover, the crossover field can be estimated by $H \sim 1/\mu$ from the classical model. The estimated cross-over field for Bi_2Se_3 is in the order of ~1T and

consistent with the MR curves in Figure 3 whereas, for the doped sample the estimated crossover field is much higher than 1T indicating the inapplicability of the classical model for the Co doped samples.

3.3.4: Hall and Magnetic Analysis

We have also investigated the magnetic properties of Co doped Bi_2Se_3 samples. Figure 4d shows the M(H) curve for all the samples. The M(H) behavior indicates that ferromagnetic ordering is induced with Co-doping in Bi_2Se_3. It is also observed that magnetization value initially increases with Co-content but with further increase of Co-content the ferromagnetism decreases indicating diluted magnetic semiconductor (DMS) like behavior (as at low temperature for 6% Co-doped the ρ(T) value increases with decrease of temperature) [72]. This observed magnetic behavior in Bi_2Se_3 is consistent with the report of Liu et al [73].

We have also carried out the Hall measurements to investigate the ferromagnetism in the Co-doped Bi_2Se_3 samples. In fact, the hysteresis loops of the Hall resistance which results from the anomalous Hall effect is the signature of the long range ferromagnetism [55], [74].The Hall resistivity in a magnetic sample is given by, $\rho_{xy}=R_HH + \rho_{AH}(M)$, where the first term is the ordinary Hall resistivity and the second term is the anomalous Hall contribution that arises from the magnetization of the material. Here H is the applied field, M is the magnetization and R_H is the ordinary Hall coefficient. Figure 3.4 (a-c) shows the magnetic field variation of Hall resistance at different temperatures for undoped and Co-doped samples. It is observed that the undoped sample shows the linear magnetic field variation of Hall resistance. As the Co content increases the non-linearity in Hall resistance is observed and for 6% Co doped the non-linearity

is maximum. Moreover, it is observed that both the saturation Hall resistance and switching field decrease with increasing temperature which is observed for the case of ferromagnetism.

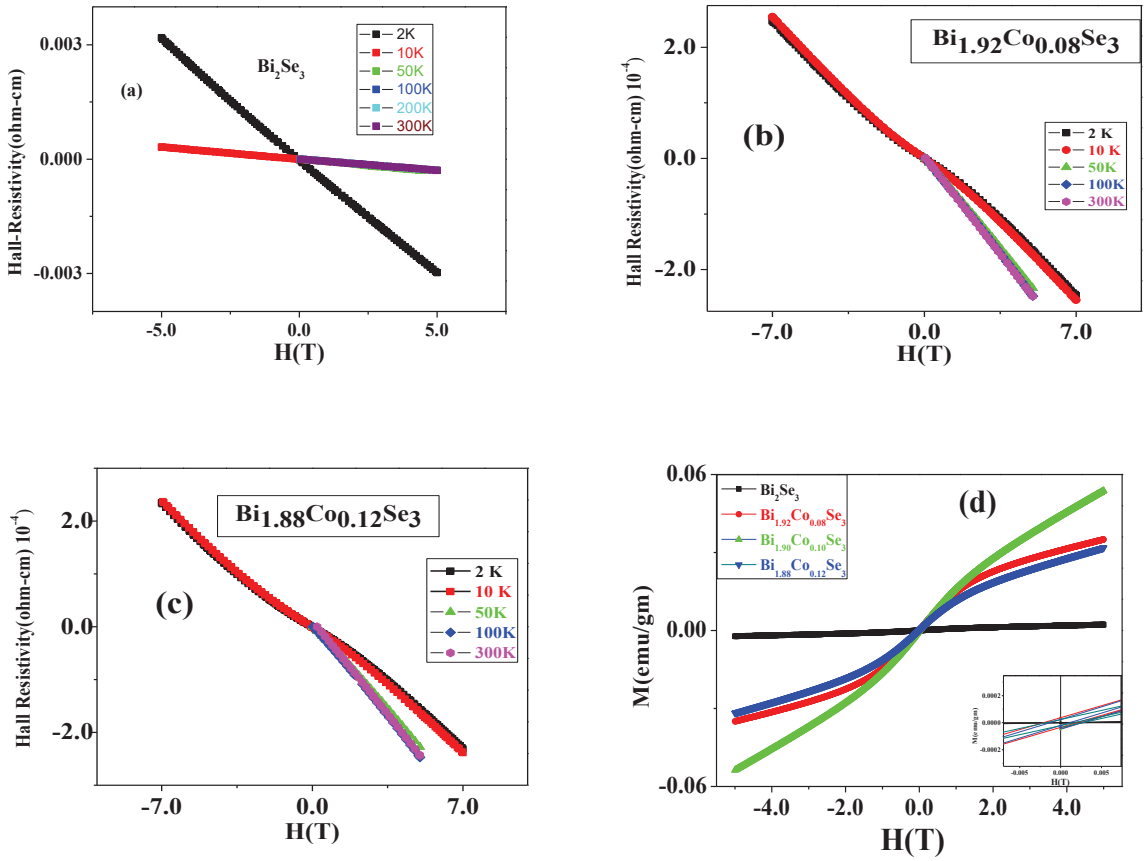

Figure 3.4: Temperature variation of Hall resistivity of $(Bi_{1-x}Co_x)_2Se_3$ [with x=0 (a), 0.04 (b), 0.06 (c)].(d) Magnetic hysteresis loops of $(Bi_{1-x}Co_x)_2Se_3$ (with x=0, 0.04, 0.05, 0.06).] Inset: The close-up view of M(H) curve to show the hysteresis loop.

From the above discussion it is clear that Co doping induces the FM order. It has also been discussed above that with Co-doping the surface energy gap opens which leads to the breaking of Time Reversal Symmetry (TRS) [73], [75]. It should be mentioned that the incorporation of magnetic impurities leads to increased disorder causing the localization in the electronic states known as WL, which is strongly related to field induced magnetization [76]. In the present investigation with 6% Co doping the MR is therefore governed by the WL effect, which suggests a long range ferromagnetic order is developed upon the alignment of magnetic

moments at low temperature and low field as is clear from the magnetic data. Moreover, as Co content increases the spectral weight suppression (SWS) also increases as Co is magnetic. It is observed initially with increase of SWS magnetization increases, but with further increase of SWS the magnetization value decreases. This indicates that when SWS is insignificant the Bi_2Se_3 behaves as diluted magnetic semiconductor (DMS). Moreover, the maximum power factor is observed when TRS is maintained. As the TRS is broken the power factor value is decreased and the peak at low temperature is also diminished. Furthermore, as the Co content increases the anomalous Hall Effect also increases and linearity in MR increases. Therefore, with the rising of Dirac cone above the Fermi level the linearity in MR and the anomalous Hall Effect increase and Power factor is decreased.

3.4 CONCLUSION

The magneto-resistance, thermopower, magnetization and Hall Effect measurements have been performed on the Co-doped Bi_2Se_3 topological insulators. It has been observed that high doping and high magnetic field raise the Dirac cone above Fermi level and leaves a gap from the valence band. The undoped sample shows the maximum MR as the destructive interference due to a π-Berry phase leads to a decrease of MR which is the key feature of topological surface states, where Dirac Fermions travel around a self intersecting path or loop due to the spins rotating in opposite ways for the different path directions and a π-Berry phase is accumulated. The consistent behavior of MR and mobility throughout the temperature range supports the applicability of Parish and Littlewood model for Bi_2Se_3, whereas, low temperature MR behavior of Co doped samples cannot be explained with the same model but can be explained with the quantum linear magneto-resistance model. Moreover, observed parabolic behavior at low magnetic field in pure Bi_2Se_3 indicates the weak antilocalization behavior.

Magnetization behavior indicates the establishment of ferromagnetic ordering with Co doping. Hall Effect data also supports the ferromagnetic behavior in Co-doped Bi_2Se_3 samples with the appearance of non-linearity. Furthermore, it is observed initially with increase of spectral weight suppression (SWS) magnetization increases, but with further increase of SWS the magnetization value decreases. This indicates that when SWS is insignificant the Bi_2Se_3 behaves as DMS. Moreover, the maximum power factor is observed when the TRS is maintained. As the TRS is broken the power factor value is decreased and the peak at low temperature is also diminished. Therefore, with the rise of Dirac cone above the Fermi level the MR and FM ordering increase and Power factor is decreased.